Journal of Membrane Science and Research 6 (2020) 367-374

Journal of Membrane Science & Research

journal homepage: www.msrjournal.com

Research Paper

Plasticization Modeling in Cellulose Acetate/NaY Mixed Matrix Membranes

Einallah Khademian [1], Mostafa Keshavarz Moraveji [2], Mitra Dadvar [2], Hamidreza Sanaeepur [3,*]

[1] Petrochemical Engineering Department, Amirkabir University of Technology (Tehran Polytechnic), Mahshahr Campus, P.O. Box 415, Mahshahr, Iran
[2] Department of Chemical Engineering, Amirkabir University of Technology (Tehran Polytechnic), Tehran, P.O. Box 15875-4413, Iran
[3] Department of Chemical Engineering, Faculty of Engineering, Arak University, Arak 38156-8-8349, Iran

Article info

Received 2020-06-04
Revised 2020-08-22
Accepted 2020-08-22
Available online 2020-08-22

Keywords

Mixed matrix membrane (MMM)
Plasticization
Modeling
Zeolite
CO_2 separation

Highlights

- Mathematical modeling of the gas permeability in the glassy polymer/nano-porous filler MMMs
- Considering the plasticization phenomenon in the presence of solid fillers
- Diffusivity and solubility of the gases in the MMMs as a function of plasticization
- Reduction of plasticization parameter (β) by increasing the filler contents at MMMs
- Antiplasticization effect of fillers by a positive shift in plasticization pressure

Graphical abstract

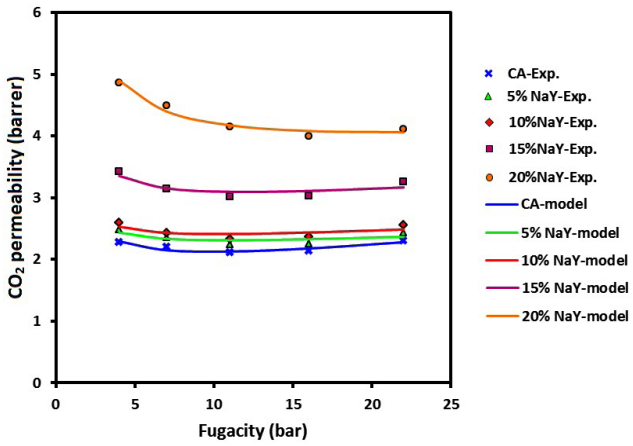

Abstract

The plasticization of mixed matrix membranes (MMMs) in the presence of solid particles differs from pure glassy polymeric membranes. This study aims to develop a mathematical model for gas permeability in the glassy polymer/nano-porous filler MMMs, considering the plasticization phenomenon in the presence of the solid particles. The diffusivity of each component is assumed to be a function of the plasticization in the presence of nano-porous fillers. The partial immobilization model with the insertion of filler contributions in gas solubility of MMMs is also applied to determine the fraction of sorbed mobile gases. In this case, the model parameters were determined by fitting the experimental data of cellulose acetate/sodium Y zeolite (CA/NaY) MMMs for CO_2/N_2 separation. The results showed that the plasticization parameter (β) is reduced by increasing the zeolite content in the MMMs, both for CO_2 and N_2 gases. The MMM plasticization declined by a shift in the plasticization pressure towards larger values. Except for the MMM with 20 wt.% NaY content, CO_2-induced plasticization fugacities of all the MMMs were best modeled with a relative error of less than 8%. Moreover, an acceptable mean relative error of 7.57% was obtained for all the MMMs containing 0-20 wt. % NaY. Statistical analysis with calculating the Pearson correlation's parameters showed a direct and strong relationship between the two coefficients C'_{HA} and b. Furthermore, it revealed a close relationship between all other coefficients, while no relationships were observed between D_0 and β, and also, F and D_0 for both the CO_2 and N_2 gases, maybe because of the small sizes of these coefficients. The zeolite particles play a role of anti-plasticizer. Additionally, by increasing the zeolite loading, the gas diffusivity variations in the membranes decreased. This reduction is another sign of the plasticization reduction in the MMMs as compared to the pure glassy membranes.

1. Introduction

Since carbon dioxide (CO_2) accounts for most of the greenhouse gas emissions, and hence, it is necessary to be separated from industrial flue gases [1, 2]. On the other hand, the captured CO_2 can be applied for enhanced oil recovery (EOR) [3-5]. Conventional methods for CO_2 separation include adsorption, absorption, cryogenic distillation, and membrane separation technology. Comparing to the other techniques, membrane separation has significant benefits including lower energy consumption, low cost, simplicity of operation, and the need for smaller equipment that makes it to be widely used in various applications [6, 7]. In the case of membrane gas separation, the high solubility of some gas components in the polymeric membrane

* Corresponding author: h-sanaeepur@araku.ac.ir; h.sanaee@yahoo.com (H. Sanaeepur)
DOI: 10.22079/JMSR.2020.128618.1394

matrices leads to an unfavorable phenomenon, the plasticization of the polymeric membranes, that it remained as a substantial challenge [8]. This decreases the separation performance of the polymeric membranes [9]. Furthermore, high pressure and, or the presence of impurities in the gas systems, reduce the separation performance of membranes [10]. Plasticization refers to a phenomenon, which is mostly dependent on the pressure originated by the dissolution of some feed components in the polymer matrix and increased mobility of the polymer chains, led to increase in the space between polymer chains and thus increase in the free volume of the membrane [11]. Regarding the solution-diffusion model, a component should first be sorbed on the membrane and then diffuse across it [12]. Plasticization of the membrane by CO_2 leads to increasing permeability and decreasing selectivity. Dissolved CO_2 swells the space between the polymer chains and leads to disruption of the polymer structure [13]. Generally, plasticization of a membrane depends on some critical factors such as membrane material, structure, thickness, feed composition, pressure, and temperature [14]. CO_2 is one of the essential plasticizer components in natural- and flue gas streams. For example, at natural gas processing at high pressures, the membrane materials adsorb 30-50 cubic centimeters of CO_2 (STP: standard temperature and pressure) per cubic centimeter of the polymer. This is equivalent to 5-10 weight percent of CO_2 in the polymer, which is resulted in a significant softening of the membrane material [15].

The permeability of a plasticizer component such as CO_2 varies when its pressure increases. This behavior is described by a dual sorption model and site saturation mechanism. At a low concentration of penetrant in the polymer matrix, microvoids in Langmuir mode are not fully saturated. As time progresses, available microvoids in Langmuir mode are almost saturated at the higher concentration of penetrant. Therefore, permeability decreases with an increase in pressure. After the available microvoids in Langmuir mode are fully saturated, more feeding of the gas at higher pressures increases the diffusion in Henry mode. Beyond that, a pressure increase leads to permeability increase; in which the corresponding pressure at this point is called the “plasticization pressure” [16].

Koros et al. [17] applied the dual-mode sorption model for mixed gas permeation across the polymeric membranes. The model could not accurately predict the permeability of the mixed gas components, due to considering no plasticization in the model. Lee et al. [18] presented a model to predict the permeability of gases in glassy polymers by considering the effect of plasticization. They found that the *diffusion coefficient* of each component depends on all other components. Also, all adsorbed gas molecules were supposed as mobile molecules. Sada et al. [19] determined the permeability of CO_2/CH_4 mixed gases in the glassy cellulose triacetate membrane. They assumed all the adsorbed gas molecules to be mobile. They concluded that the presence of CH_4 in the mixture decreases the CO_2 permeability. CH_4 induces an antiplasticization effect against the CO_2-induced plasticization behavior. Visser et al. [20] also applied the dual sorption model to determine the permeability of mixed gas components in glassy polymers. They studied the trade-off between competitive sorption and plasticization effect in hollow fiber membranes. They concluded that an inert gas, which presents in simultaneous with CO_2 in the feed mixture, occupies the available microvoids in Langmuir mode. Therefore, the adsorption rate of CO_2 molecules decreases, which means the reduction of plasticization. Saberi et al. [21] proposed a model for predicting the diffusivity of mixed gas components in asymmetric glassy cellulose acetate membrane in the presence of plasticization. Permeances of the feed gas components as compared to those for the pure gases were declined that could be attributed to occupying the Langmuir sites with the second component, and thus, a decrease in gas sorption. Also, they calculated the immobilization factor (F) for CO_2 and CH_4 and showed that it decreases for CO_2 with an increase in second component (CH_4) fraction due to a reduction in plasticization. Additionally, they concluded that the effective diffusivity of pure CO_2 is significantly pressure dependent, and this dependency is almost disappeared with the increase in CH_4 content of the feed.

This study presents a mathematical model for the plasticization, which is induced by the (CO_2 and N_2) gas permeation in an MMMs. Briefly, it should be notified that MMMs are composed of inorganic/organic fillers dispersed in the polymeric matrix of the membranes. They combine both the advantages of inorganic and organic materials to overcome the permeability/selectivity trade-off of the present polymeric membranes. In recent decades, MMMs have been attracted more attention, and it is expected to replace traditional membranes shortly [22-25]. In the present model, the dual sorption model is applied to predict the permeability of CO_2 and N_2 gases. A concentration-dependent diffusion coefficient is considered in the presented model. Moreover, based on the partial immobilization model, it is assumed that the fractions of the gases adsorbed in the Langmuir sites are mobile while the remaining fractions are immobile. Also, the present model considers the effect of solid particles dispersed into the polymer matrix on the gas components-induced plasticization. Using our previous data for pure CO_2 and N_2 permeations in glassy cellulose acetate/nano-porous sodium Y zeolite (CA/NaY) MMMs [26], the effect of different NaY loadings (0-20 wt.%) into the MMMs is investigated, and the corresponding plasticization pressures are determined. This is a characteristic feature of this work that distinguishes from the others; it takes into account the effect of different amounts of solid zeolite particles loaded in the membrane matrix on the plasticization which is induced by the gas components.

2. Theory and modeling

Barrer [27] proposed two mechanisms that involve in the transport of species through the glassy polymers with several micropores in their matrices:

1. Solution based on Henry's law
2. Hole filling, based on the Langmuir theory

This type of sorption is called the dual-mode sorption model. The sorption isotherm for pure gas component A based on the dual-mode sorption model is considered as follows [28]:

$$C_A = C_{DA} + C_{HA} = K_{DA}\, p_A + \frac{C'_{HA} b_A\, p_A}{1 + b_A\, p_A} \tag{1}$$

C_A is the volumetric concentration of gas A in the polymer (cm^3(STP)/cm^3 polymer), C_{DA} represents the concentration of dissolved gas A based on Henry's law, C_{HA} denotes the concentration of dissolved gas A in the Langmuir area, K_{DA} is Henry’s coefficient, C'_{HA} represents pore saturation constant, b_A is the affinity constant of pores and p_A represents the partial pressure of A component. In Eq. (1), the first term represents common dissolution in Henry’s area, and the second term represents sorption in the micropores.

In the dual-mode sorption, it is assumed that the model parameters do not depend on the pressure [29]. A limitation of the dual-mode sorption model is the calculation of sorption parameters using the experimental data [28]. In the case of glassy polymer-based MMMs, further challenges will be comprised due to the presence of filler particles; Eq. (1) has presented for the pure glassy polymeric membranes; based on the formula given by Paul and Kemp [30] for the MMMs, Eq. (1) can be modified to Eq. (2) to take into account the effect of zeolite (NaY) particles in the cellulose acetate (CA) polymer matrix:

$$C_A = \phi_P C_{DA} + \phi_D C_{HA} = \phi_P K_{DA}\, p_A + \phi_D \frac{C'_{HA} b_A\, p_A}{1 + b_A\, p_A} \tag{2}$$

where ϕ_P and ϕ_D represent the volumetric fractions of the polymer and dispersed filler, respectively. Similarly, an equation can be written for pure gas component B. Then, the solubility for pure gas components A and B can be determined by the following equation [31]:

$$S_A = \frac{C_A}{p_A} \quad ; \quad S_B = \frac{C_B}{p_B} \tag{3}$$

If downstream (permeate) pressure is ignored in comparison with the upstream (feed) pressure, the permeability of the pure gas A in a glassy polymer from Eq. (2) can be determined in steady-state condition based on the dual-mode sorption and dual-mode mobility models [32]:

$$P_A = \phi_p K_{DA} D_{DA} + \frac{\phi_d C'_{HA} b_A D_{HA}}{1 + b_A\, p_A} \tag{4}$$

In this equation, D_{DA} and D_{HA} are diffusion coefficients in Henry’s and Langmuir’s modes, respectively.

Regarding the partial immobilization model, a fraction of gas sorbed in the Langmuir mode is mobile. Paul and Koros [32] showed that the penetrants in the Langmuir microvoids have less mobility while they are fully mobile at Henry’s mode. Therefore, they introduced parameter F, which indicates a fraction of mobile components at Langmuir’s mode. The remaining other fraction of components at Langmuir’s mode, *1-F*, is immobile. Thus, F is called the immobilization factor, which depends on the nature of the polymer-diffusive component and the temperature [33].

Diffusion of component A in the presence of plasticization is defined as follows [34]:

$$D_A(C_{mA}) = D_{A0}\exp(\beta_A C_{mA}) \quad (5)$$

where D_{A0} represents pure gas diffusivity when $C_{mA} \to 0$. C_{mA} refers to the concentration of the mobile gas species. β_A that is called the plasticization parameter, is an experimental constant that depends on the nature of the diffusive component-polymer system, temperature, and thickness of the membrane. β_A is a representative for the plasticization capability of the diffusive material [29, 35]. Due to the plasticization of polymer chains, the gas permeabilities at high pressure deviates from the dual sorption model [20]. Ideal selectivity of the two components is calculated by dividing the pure gas permeabilities as follows [36]:

$$\alpha_{AB} = \frac{P_A}{P_B} \quad (6)$$

where P_A and P_B are the permeability of pure gases *A* and *B*, respectively.

Finally, the permeability and effective diffusivity of *A* (CO_2) and *B* (N_2) in terms of pressure for glassy polymers, which are described by [21], should be modified to consider the effect of zeolite (NaY) particles on softening or plasticization phenomena (Eqs. 7-10 with parameters ϕ_p and ϕ_d). ϕ_d represents the contribution of NaY particles in the gas sorption (in addition to sorption in the Langmuir area).

$$P_A = \frac{D_{A0}}{\beta_A p_{A2}}\left\{\exp\left[\beta_A\left(\phi_p K_{DA} + \frac{\phi_d F A C'_{HA} b_A}{1 + b_A p_{A2}}\right)p_{A2}\right] - 1\right\} \quad (7)$$

$$D_{eff,A} = D_{A0}\exp\left[\beta_A\left(\phi_P K_{DA} + \frac{\phi_d F A C'_{HA} b_A}{1 + b_A p_{A2}}\right)p_{A2}\right]\left[\frac{\phi_P K_{DA} + \frac{\phi_d F A C'_{HA} b_A}{(1 + b_A p_{A2})^2}}{\phi_P K_{DA} + \frac{\phi_d C'_{HA} b_A}{(1 + b_A p_{A2})^2}}\right] \quad (8)$$

$$P_B = D_{B0}\left\{\exp\left[\beta_B p_{A2}\left(\phi_p K_{DA} + \frac{\phi_d F A C'_{HA} b_A}{1 + b_A p_{A2}}\right)\right]\left(\phi_p K_{DB} + \frac{\phi_d F B C'_{HB} b_B}{1 + b_A p_{A2}}\right)\right\} \quad (9)$$

$$D_{eff,B} = D_{B0}\exp\left[\beta_B\left(\phi_p K_{DA} + \frac{\phi_d F A C'_{HA} b_A}{1 + b_A p_{A2}}\right)p_{A2}\right]\left[\frac{\phi_p K_{DB} + \frac{\phi_d F B C'_{HB} b_B}{(1 + b_B p_{B2})^2}}{\phi_p K_{DB} + \frac{\phi_d C'_{HB} b_B}{(1 + b_B p_{B2})^2}}\right] \quad (10)$$

D_{eff} is the effective diffusivity and p_{A2} and p_{B2} are upstream pressures for A and B gases. It is worth mentioning that the experimental data of permeabilities are obtained at a high-pressure range of 4 to 22 bar [26]; therefore, a modified pressure (or fugacity) will be applied here. For fugacity calculations, the Soave-Redlich-Kwong (SRK) equation of state is considered at the process conditions.

3. Results and discussion

To validate the present model, the model predictions were compared with the permeability of CO_2 and N_2 pure gases in the CA/NaY (0-20 wt%) MMMs [26]. In this case, the parameters in Eq. (4) were calculated by nonlinear least squares (NLLS) fitting of the pure CO_2 and N_2 permeability data. The obtained parameters from Eq. (4) were used in Eqs. (7) and (9), then parameters β, F, and D_0 for CO_2 and N_2 were determined by fitting the resultant equations and the experimental data.

Also, for solubility calculations, first the obtained parameters in Eq. (4) were substituted in Eq. (2), and then the gas solubility coefficients were determined from Eq. (3).

3.1. Comparison of fugacity and pressure with SRK equation of state

The SRK equation of state has been used to obtain fugacity. Figure 1 shows the relationship between fugacity and pressure for CO_2 and N_2 gases. According to the results, the difference between pressure and fugacity can be neglected for N_2, and hence, it can be considered as an ideal gas in the pressure range of 4-22 bar. However, it cannot consider CO_2 as an ideal gas where a mean deviation of 5% is observed between the corresponding CO_2 fugacities and pressures, so the following calculations for CO_2 would be accomplished in terms of fugacity.

3.2. Studying the model parameters and the effect of solid fillers on membrane plasticization

Plasticization modeling in MMMs through the dual sorption model requires the permeability data at different pressures. Here, the experimental data of Sanaeepur et al. [26] were used for adjusting the model parameters. The obtained parameters for the dual sorption model (Eq. (4)) are given in Table 1. It should be noted that the parameters obtained for this model were calculated using nonlinear least square (NLLS) regression technique with the MATLAB software. In the dual sorption model (Eq. (4)), the larger Henry's coefficient (K_D), Langmuir saturation constant (C'_H), and affinity constant of the pores (b) are, the higher gas solubility will be [37].

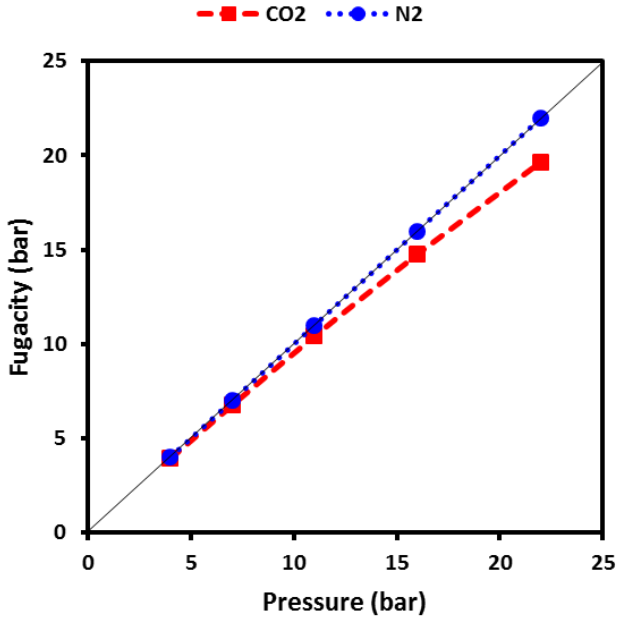

Fig. 1. The relationship between fugacity and pressure for CO_2 and N_2 gases.

Regarding Table 1, the higher values of these coefficients for CO_2 to N_2 indicate higher sorption of CO_2. In the dual sorption model ((Eq. (4)), Henry's coefficient (K_D) and saturation constant of pores (C'_H) increase with increasing the condensation of gases [38]. Since the condensability of CO_2 is greater than N_2 (from comparing the critical temperatures and the Lenard-Jones energy parameters [39-41]), the sorption coefficients of CO_2 is greater than N_2 as shown in Table 1. The value of 1.473 cm^3(STP)/(cm^3(polymer).bar^1) for solubility coefficient from the Henry's law (K_D) for pure CA membrane in Table 1 is comparable with that of reported by Saberi et al. [21], i.e. 1.43 cm^3(STP).cm^{-3}(polymer).bar^{-1}. With an increase in the NaY zeolite content, the free spaces between the solid filler and the polymer increase. However, a free volume between the polymer chains can decrease as the polymer chains become more rigid. It could be more intensified here, whereas the membrane samples annealed. These two phenomena do not contradict each other. However, this is the space between the micron-sized solid filler and the polymer that overcomes the decline in free volume and leads to greater permeability of the MMMs. The interfacial gap between zeolite particles and the polymer matrix can increase the sorption coefficient of Henry's law (K_D). However, a different behavior was observed for the Langmuir constants (C'_H and b, Eq. (4)) in the presence of NaY zeolite particles. To analyze the Langmuir parameters of the dual sorption model (Eq. (4)), it should be noted that the CA/NaY MMMs have annealed at 150 °C (a temperature below the cellulose acetate glass transition temperature). Annealing a glassy membrane leads to the formation of a better morphology, diminishing the microscopic cracks in its structure, and hence, will result in a more favorable separation performance. Annealing the membranes causes the relaxation of the polymer chains and reduction of excess free volume. Also, because of the compressibility of the membrane structure, it has a great impact on the sorption parameters. For example, Langmuir adsorption capacity (C'_H) in an annealed membrane is lower than that of the membrane made at room temperature, due to the reduction of excess free volume [42]. Hiroshi et al. [43], Hachisuka et al. [44], and Okamoto et al. [37] discussed the effect of membrane annealing on sorption parameters. They concluded that annealing a glassy membrane reduces the sorption parameters due to a decline in micron volumes inside the polymer. However, in the case of glassy cellulose acetate membranes, Sanaeepur et al. [26] stated that through the annealing near glass transition temperature, polymer chains are toughened because of the methylene bond formations between the cellulose polymer chains. As the results confirmed by XRD analysis, the inter-chain spaces were reduced through the annealing. This can be the reason for lower sorption parameters which are obtained here based on the work by Sanaeepur et al. [26] as compared to those of Saberi et al. [21].

One of the frequently used measures of linear dependence between two random variables is the Pearson correlation coefficient. This is defined for two variables X and Y as the covariance of the two variables divided by the product of their standard deviations (which acts as a normalization factor). It can be expressed by r_{XY}, as:

$$r_{XY} = \sum_{i=1}^{n} \frac{X_i - \overline{X}}{\sqrt{\sum_{k=1}^{n}\left(X_k - \overline{X}\right)^2}} \cdot \frac{Y_i - \overline{Y}}{\sqrt{\sum_{k=1}^{n}\left(Y_k - \overline{Y}\right)^2}} \quad (11)$$

where $\overline{X} = \frac{1}{n}\sum_{i=1}^{n} X_i$ is the mean of X. The coefficient r_{XY} ranges from -1 to 1 and it is invariant to linear transformations of either variables. r_{XY} values close to 1 indicate a positive relationship between X and Y, while the values close to -1 stand for a negative (inverse) relationship. A value close to 0 shows the absence of a relationship between two variables. It should be noted that the r_{XY} cannot be computed when one or both variables are constant, since the quantity $\sqrt{\sum_{k=1}^{n}\left(X_k - \overline{X}\right)^2}$ is 0, and thus, the Pearson correlation coefficient is undetermined [45].

Using SPSS software, the statistical calculations related to Pearson correlation were done and the results were summarized in Table 2. According to Table 2, there is a direct and strong relationship between the two coefficients C'_{HA} and b. Of course, there is a close relationship between all other coefficients.

Langmuir adsorption capacity (C'_H) increases by increasing the NaY zeolite contents due to the increase in zeolite sorption sites. Affinity constant of pores (b) represents the sorption rate of gas in micropores over the desorption rate [46]. It has higher values for CO_2 compared to N_2 (Table 1), which reveals a higher affinity of pores for adsorbing the CO_2 molecules. It can also be observed that the values of affinity constants increase at higher loadings of porous fillers due to the increased number of sorption sites.

It has been illustrated that the more gas sorption rate, the more gas-induced plasticization will be [34]. This is also evident from the plasticization parameters calculated by the model and illustrated in Table 3. The parameter β, which is a representative of gas-induced plasticization, is greater for CO_2 than N_2. The higher parameter β the lower concentration of the gas is needed to plasticize the membrane [47]. The value of 0.0336 for parameter β of the pure CA membrane differs from that of equals 0.086 for Saberi et al. [21] which can be attributed to the membrane annealing at a temperature near the glass transition temperature which reduces the plasticization of CA. Moreover, the data by Saberi et al. [21] was for the mixed gas permeation that differs from pure gas results, due to the competitive sorption of mixed gas components into the membrane micropores [48].

In the case of plasticization parameters of the MMMs for both the CO_2 and N_2 in Table 3, a dual sorption model was used, and the effect of membrane plasticization under excessive sorption of CO_2 was considered using the β factor. As can be seen, by increasing the NaY zeolite content, plasticization parameter β decreases, which indicates a positive effect of the particles in preventing gas-induced plasticization in the MMMs. Adding the zeolites in the polymer matrix is followed by intermolecular interactions between the zeolites and polymer matrix that can restrict the polymer chains' motions around the particles. The zeolite particles can play an antiplasticization role. Also, membrane annealing can diminish the unwanted fine cracks which are formed during the membrane preparation. As a result, excessive sorption of gases, and consequently, the plasticization of the MMMs were reduced with the increase in zeolite loadings.

F factor represents the ratio of diffusivity in micropores over the diffusivity in the polymer matrix. As can be seen in Table 3, F values for CO_2 are greater than N_2, which means CO_2 has more mobility in NaY zeolite particles. It can be attributed to high sorption of CO_2 in the micropores, on the surface and microchannels of the zeolites. F values increases for CO_2 up to 10 wt.% NaY loading due to the increase in CO_2 mobility, while it decreases at 15 wt.% NaY loading. The reduction in F is due to agglomeration of the particles, which affects the diffusion of the gas molecules into the micropores, and consequently, reduces the permeation inside the pores. The agglomeration phenomenon is more evident from the results of 20 wt.% NaY loading. Generally, for F values close to unity, the presumption of partial immobilization is suitable, while the overall immobilization model is applied for lower F values. N_2 transport across the membrane is diffusion-controlled rather than to be solubility-controlled. D_0 increases with the increase in NaY zeolite contents. The more NaY loading, the more diffusion of N_2 will occur. However, the D_0 values for CO_2 are higher than those for the N_2. It is due to the lower kinetic diameter of CO_2 molecules as compared to N_2. On the other hand, CO_2 has benefited a further transport mechanism than the N_2 due to adequate sorption in the zeolite pores. The concentration of initial adsorbed layers of CO_2 at the surface and within the zeolite pores can raise a concern about the controlled diffusion of the remaining gas into the zeolite. Therefore, as compared to pure CA membrane, it can be observed that D_0 of the CA/NaY MMMs reduces for low zeolite contents (< 10 wt.%), and then increases again at 15 wt.% NaY and more, due to the increase in free volumes of the MMMs. According to Table 4, which summarizes the calculated Pearson coefficients by SPSS software, there are no relationships between D_0 and β, and also, F and D_0 for both the CO_2 and N_2 gases, maybe because of the small sizes of these coefficients. Moreover, for N_2, there is a negative (inverse) relationship between β and F.

Table 1
The obtained parameters from the dual sorption model (Eq. (4)) for CO_2 and N_2 in CA/NaY MMMs.

Component	NaY zeolite loading (wt.%)	K_D $\left(\frac{cm^3(STP)}{cm^3.bar}\right)$	C'_H $\left(\frac{cm^3(STP)}{cm^3}\right)$	b (bar^{-1})
CO_2	0	1.473	2.014	3.501
	5	1.546	8.762	5.261
	10	1.626	9.494	12.245
	15	1.880	14.685	15.061
	20	2.068	17.647	22.566
N_2	0	0.306	0.802	0.054
	5	0.342	1.104	0.091
	10	0.354	1.192	0.095
	15	0.356	2.745	0.330
	20	0.420	3.029	0.476

Table 2
The Pearson coefficients for the dual sorption model parameters (Eq. (4)) for CO_2 and N_2 in CA/NaY MMMs.

		$C'_H\left(\frac{cm^3(STP)}{cm^3}\right)$	b (bar^{-1})
CO_2	$K_D\left(\frac{cm^3(STP)}{cm^3.bar}\right)$	0.946	0.967
	$C'_H\left(\frac{cm^3(STP)}{cm^3}\right)$	1	0.926
N_2	$K_D\left(\frac{cm^3(STP)}{cm^3.bar}\right)$	0.821	0.876
	$C'_H\left(\frac{cm^3(STP)}{cm^3}\right)$	1	0.982

Table 3
The calculated plasticization parameters of Eqs. (7) and (9) for CO_2 and N_2 permeabilities in CA/NaY MMMs.

Component	NaY zeolite loading (wt.%)	β	F	D_0 (cm^2/s) $\times 10^{+9}$
CO_2	0	0.0336	0.858	1.155
	5	0.0243	0.864	1.153
	10	0.0170	0.919	1.132
	15	0.0130	0.804	1.273
	20	0.0028	0.460	1.829
N_2	0	0.0043	0.018	0.2831
	5	0.0031	0.033	0.3276
	10	0.0019	0.274	0.3297
	15	0.0004	0.967	0.4035
	20	0.0001	0.421	0.4216

Table 4
The Pearson coefficients for the plasticization parameters (Eqs. (7) and (9)) for CO_2 and N_2 permeabilities in CA/NaY MMMs.

Component		F	D_0
CO_2	β	0.743	0
	F	1	0
N_2	β	- 0.807	0
	F	1	0

3.3. Gas diffusivity in terms of fugacity

Variations in the diffusivity of CO_2 and N_2 in the MMMs in terms of fugacity were calculated based on Eqs. (8) and (10) for different NaY zeolite loadings (0-20 wt.%) and depicted in Figures 2 and 3. By increasing the gas fugacity, its sorption, and in turn, the plasticization of the membrane increases. Plasticization increases the space between polymer chains. As a result, the penetration rate of the gas components increases by the plasticization-induced free volume increase [49]. This increases the diffusion of both gases into the membranes. However, the diffusion of a gas with higher sorption is more influenced by the fugacity changes. Thus, according to the more adsorption of condensable CO_2 gas, a higher effect of fugacity on the diffusivity for CO_2 rather than N_2 is predictable. As shown in Figures 2 and 3, at fugacities near 11 bar and more, the positive growth of diffusivity for CO_2 is greater than N_2, which can increase the CO_2/N_2 diffusivity selectivity.

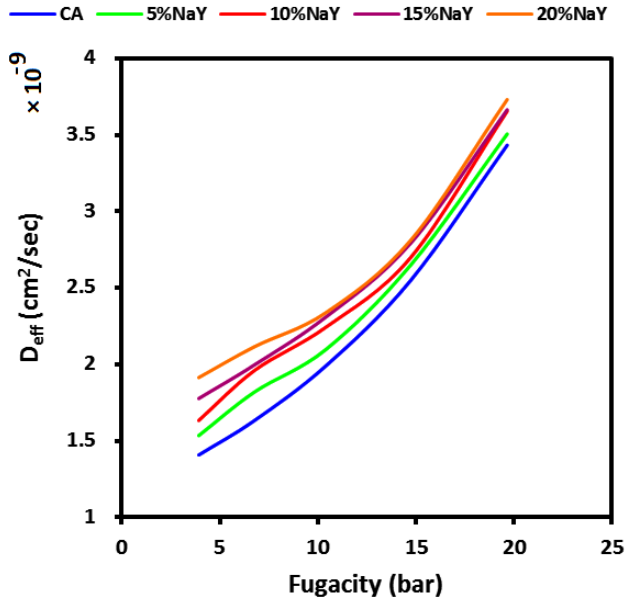

Fig. 2. The CO_2 effective diffusivity in the MMMs in terms of fugacity.

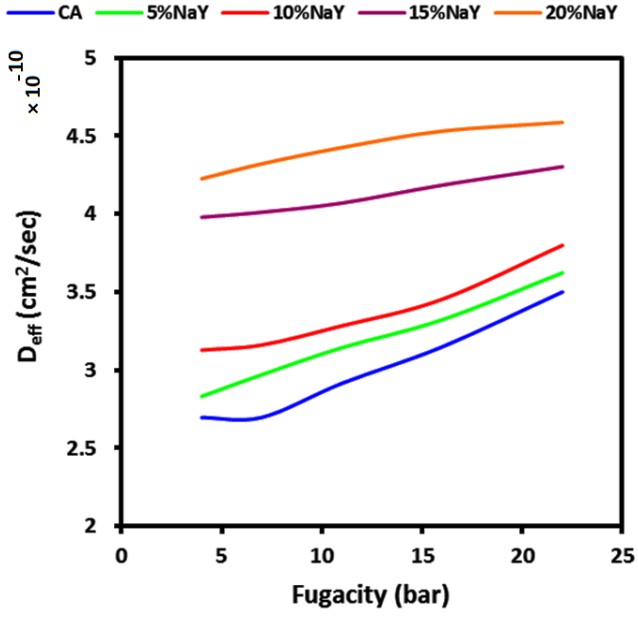

Fig. 3. The N_2 effective diffusivity in the MMMs in terms of fugacity.

3.4. Gas solubility in terms of fugacity

Figures 4 and 5 depict solubility of CO_2 and N_2 in pure CA and CA/NaY MMMs with different NaY zeolite contents in terms of fugacity. As can be seen in Figure 4, the solubility of all the membranes has a slight descending behavior with the fugacity increase, especially in the higher fugacities. For all the membranes, at lower CO_2 fugacities, solubility has significantly decreased because the microvoids in the Langmuir area and also the zeolite voids are not saturated. Therefore, the lower is the fugacity, and the higher is the solubility. Solubility decreases at higher fugacities due to the occupation of Langmuir sites by the gas molecules. Also, increasing the NaY contents in the MMMs leads to an increase in Langmuir sites and gas solubility. However, through the solubility increases, the membranes are exposed to more softening or plasticization. On the other hand, more polymer-particle interactions at higher zeolite loadings solidify the polymer chains around the particles and enhance the effect of anti-plasticization. As seen in Figure 5 for N_2 solubility in terms of fugacity, a behavior almost the same as CO_2 (Figure 4) is observed.

Comparing the results of Figures 4 and 5 with Figures 2 and 3, it can be found that with the increment in fugacity, a higher increasing rate is observed for diffusivity in comparison with the solubility. Moreover, by increasing the zeolite contents in the polymer matrix, the increase in diffusivity is lower than the solubility for both gases.

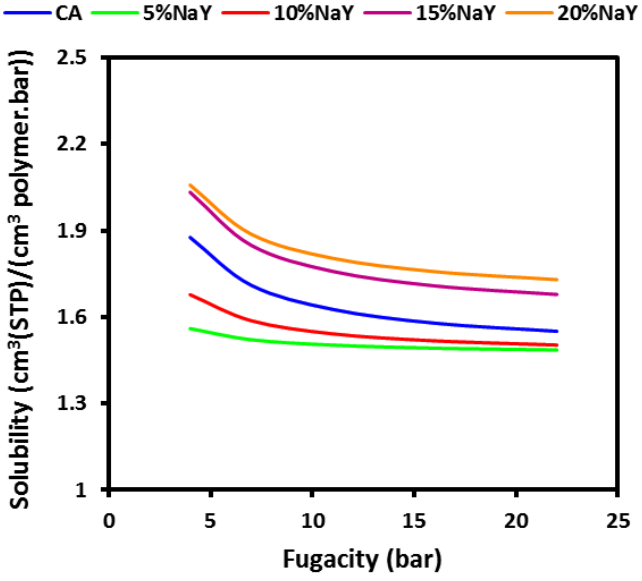

Fig. 4. The CO_2 solubility in the pure and MMMs in terms of fugacity.

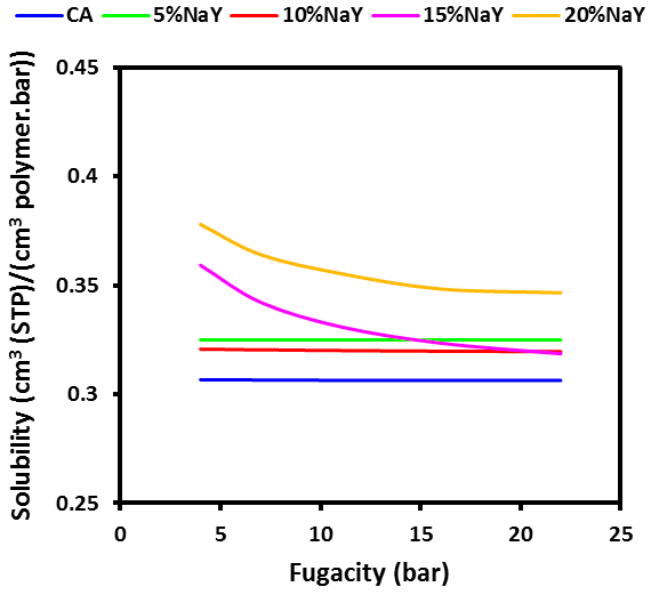

Fig. 5. The N_2 solubility in the pure and MMMs in terms of fugacity.

3.5. Permeability and selectivity in terms of fugacity

Variations in the CO_2 permeability in terms of fugacity were calculated based on the dual sorption model for different NaY zeolite loadings (0-20 wt.%) and presented in Figure 6. As mentioned above, the plasticization pressure is a pressure where the gas permeability in a glassy membrane reaches its minimum value. At pressures higher than the plasticization pressure, volume relaxation in the form of dilation or swelling of the polymer has been observed [50]. On the other hand, at pressures lower than the plasticization pressure, the gas sorption rate in the polymer is less than the swelling rate of the polymer matrix due to the adsorbed gas. This inequality increases by increasing the pressure up to the plasticization value. Then, at the plasticization pressure, polymer entanglements which are the points in the polymer matrix with a high chain density are dilated. With further increase in the pressure, the inequality is reversed [51]. But in the case of MMMs, as mentioned previously, an opposite effect of the antiplasticization of polymer chains in the presence of zeolite particles affects the inequality. Therefore, the zeolite filler-induced antiplasticization could shift the plasticization pressure of the MMM to a larger value as compared to the pure polymer. In fugacities less than the plasticization fugacity, according to the saturation mechanism of Langmuir sites, permeability decreases through filling the pores and saturating sites. Since the gases with higher condensation capability are more adsorbed, CO_2 is more affected by the fugacity than the N_2 is. As shown in Figure 7 for CO_2/N_2 selectivity, a behavior very similar to permeability is observed.

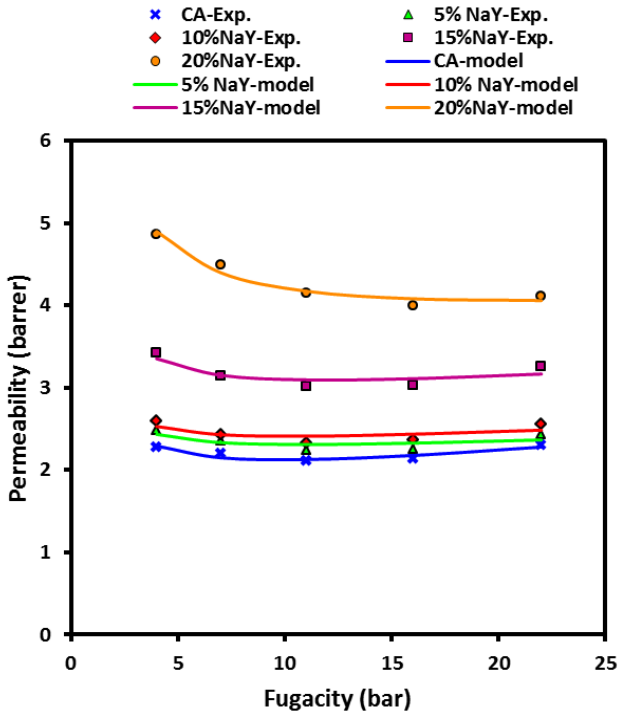

Fig. 6. The CO_2 permeability in the MMMs in terms of fugacity.

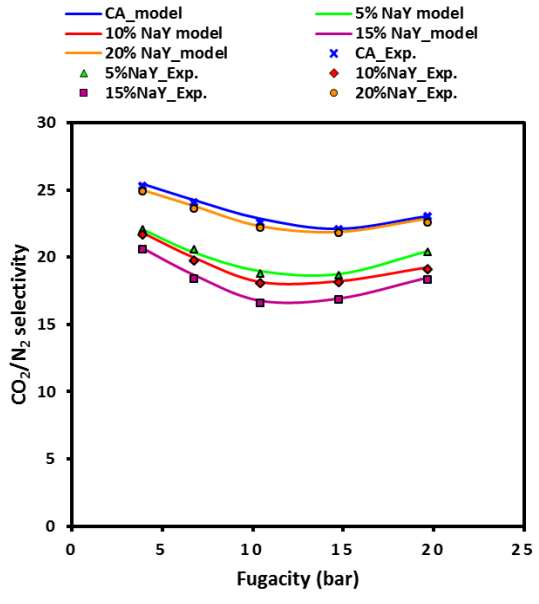

Fig. 7. The effect of fugacity on the CO_2/N_2 selectivity.

3.6. A comparison between the plasticization fugacity of the model results with the experimental data

The plasticization fugacity for various NaY zeolite contents in the MMMs was calculated via MATLAB software and compared with the experimental data. Sanaeepur et al. [26], using the second-order polynomials have fitted the permeability data in terms of pressure for pure CA membrane and the CA/NaY MMMs, to calculate the CO_2-induced plasticization pressures. Here, the plasticization pressure values by Sanaeepur et al. [26] were converted to fugacities to be compared by the model results (Table 5). Except for the MMM with 20 wt.% NaY content, CO_2-induced plasticization fugacities of all the MMMs were best modeled with a relative error of less than 8%. Also, an acceptable mean relative error of 7.57% was obtained for all the MMMs containing 0-20 wt. % NaY.

Table 5
A comparison between the CO_2-induced plasticization fugacities in the pure CA and CA/NaY MMMs calculated by the model with the experimental data.

Membrane	Plasticization fugacity (bar)		Error (%)
	Sanaeepur et al. [26]	Model	
CA	11.97	11.12	7.10
CA/NaY 5 wt.%	12.54	11.57	7.74
CA/NaY 10 wt.%	12.32	11.64	5.52
CA/NaY 15 wt.%	12.92	12.37	4.26
CA/NaY 20 wt.%	14.13	16	13.23
		Mean	7.57

4. Conclusions

In this work, the basic dual-mode (Henry-Langmuir) sorption model was applied and developed to model the gas-induced plasticization phenomenon in the mixed matrix membranes (MMMs). First, the permeability variations for CO_2 and N_2 in terms of pressure were determined. Pearson correlation is a statistical technique for investigating the relationship between two quantitative, continuous variables. The calculated Pearson's parameters demonstrated a direct and strong relationship between the two coefficients C'_{HA} and b. Of course, there was a close relationship between all other coefficients. There were no relationships between D_0 and β, and also, F and D_0 for both the CO_2 and N_2 gases, maybe because of the small sizes of these coefficients. To obtain the plasticization pressures of the MMMs, minimum values of permeability in terms of pressure (fugacity) at various filler contents were calculated, and the results were compared with the previous work by Sanaeepur et al. [26], which provided for cellulose acetate/nano-porous sodium zeolite Y (CA/NaY) MMMs. Good conformity between the model and experimental data of plasticization pressure was observed with a reasonable mean relative error of 7.57%.

Abbreviations

b_A	affinity constant of pores for A component (bar^{-1})
C_A	volumetric concentration of gas A in the polymer (cm^3(STP)/cm^3 polymer)
C_{DA}	concentration of dissolved gas A based on Henry's law (cm^3(STP)/cm^3 polymer)
C_{HA}	concentration of dissolved gas A in the Langmuir area (cm^3(STP)/cm^3 polymer)
C'_{HA}	pore saturation constant for A component (cm^3(STP)/cm^3 polymer)
C_{mA}	Concentration of the mobile gas species for A component (cm^3(STP)/cm^3 polymer)
D_{A0}	pure gas diffusivity for A component when $C_{mA} \to 0$ (cm^2/s)
D_{eff}	effective diffusivity (cm^2/s)
D_{DA}	diffusion coefficients in Henry's mode for A component (cm^2/s)
D_{HA}	diffusion coefficients in Langmuir's mode for A component (cm^2/s)
F	immobilization factor
K_D	Henry's coefficient (cm^3(STP)/(cm^3.bar^1))
p_A	partial pressure of A component (bar)
p_{A2}	upstream pressure (bar)
P_A	permeability of pure gas A (cm^3 (STP) cm/(cm^2 cmHg s))
P_B	permeability of pure gas B. (cm^3 (STP) cm/(cm^2 cmHg s))
MMM	mixed matrix membrane
r_{XY}	Pearson correlation coefficient of two variables
S_A	solubility for pure gas components A (cm^3(STP)/(cm^3 polymer.bar))
S_B	solubility for pure gas components B (cm^3(STP)/(cm^3 polymer.bar))
X	variable of Pearson correlation
$\overline{X}$	mean of X
Y	variable of Pearson correlation
$\overline{Y}$	mean of Y
α_{AB}	ideal selectivity of the two components A and B
β_A	component A-induced plasticization parameter
ϕ_P	volumetric fractions of the polymer
ϕ_D	volumetric fractions of the dispersed filler

References

[1] H. Sanaeepur, R. Ahmadi, A. Ebadi Amooghin, D. Ghanbari, A novel ternary mixed matrix membrane containing glycerol-modified poly(ether-block-amide) (Pebax 1657)/copper nanoparticles for CO_2 separation, J. Membr. Sci., 573 (2019) 234-246. https://doi.org/10.1016/j.memsci.2018.12.012.

[2] S. Sanaeepur, H. Sanaeepur, A. Kargari, M.H. Habibi, Renewable energies: climate-change mitigation and international climate policy, Int. J. Sustain. Energy, 33 (2014) 203-212. https://doi.org/10.1080/14786451.2012.755978.

[3] O. Hosseinkhani, A. Kargari, H. Sanaeepur, Facilitated transport of CO_2 through Co(II)-S-EPDM ionomer membrane, J. Membr. Sci., 469 (2014) 151-161. https://doi.org/10.1016/j.memsci.2014.06.021.

[4] H. Sanaeepur, A. Ebadi Amooghin, A. Moghadassi, A. Kargari, Preparation and characterization of acrylonitrile–butadiene–styrene/poly(vinyl acetate) membrane for CO_2 removal, Sep. Purif. Technol., 80 (2011) 499-508. https://doi.org/10.1016/j.seppur.2011.06.003.

[5] I. Khalilinejad, A. Kargari, H. Sanaeepur, Preparation and characterization of (Pebax 1657+silica nanoparticle)/PVC mixed matrix composite membrane for CO_2/N_2 separation, Chem. Pap., 71 (2017) 803-818. https://doi.org/10.1007/s11696-016-0084-5.

[6] A. Brunetti, F. Scura, G. Barbieri, E. Drioli, Membrane technologies for CO_2 separation, J. Membr. Sci., 359 (2010) 115-125. https://doi.org/10.1016/j.memsci.2009.11.040.

[7] A. Ebadi Amooghin, S. Mirrezaei, H. Sanaeepur, M.M.M. Sharifzadeh, Gas permeation modeling through a multilayer hollow fiber composite membrane, J. Membr. Sci. Res., 6 (2020) 125-134. 10.22079/jmsr.2019.112328.1281.

[8] H. Sanaeepur, A. Ebadi Amooghin, S. Bandehali, A. Moghadassi, T. Matsuura, B. Van der Bruggen, Polyimides in membrane gas separation: Monomer's molecular design and structural engineering, Prog. Polym. Sci., 91 (2019) 80-125. https://doi.org/10.1016/j.progpolymsci.2019.02.001.

[9] H. Sanaeepur, S. Mashhadikhan, G. Mardassi, A. Ebadi Amooghin, B. Van der Bruggen, A. Moghadassi, Aminosilane cross-linked poly (ether-block-amide) (PEBAX 2533): Characterization and CO_2 separation properties, Korean J. Chem. Eng., 36 (2019) 1339-1349. 10.1007/s11814-019-0323-x.

[10] A. Bos, I.G.M. Pünt, M. Wessling, H. Strathmann, CO_2-induced plasticization phenomena in glassy polymers, J. Membr. Sci., 155 (1999) 67-78. https://doi.org/10.1016/S0376-7388(98)00299-3.

[11] A.L. Ahmad, J.K. Adewole, C.P. Leo, S. Ismail, A.S. Sultan, S.O. Olatunji, Prediction of plasticization pressure of polymeric membranes for CO_2 removal from natural gas, J. Membr. Sci., 480 (2015) 39-46. https://doi.org/10.1016/j.memsci.2015.01.039.

[12] K.L. Gleason, Z.P. Smith, Q. Liu, D.R. Paul, B.D. Freeman, Pure-and mixed-gas permeation of CO_2 and CH_4 in thermally rearranged polymers based on 3, 3′-dihydroxy-4, 4′-diamino-biphenyl (HAB) and 2, 2′-bis-(3, 4-dicarboxyphenyl) hexafluoropropane dianhydride (6FDA), J. Membr. Sci., 475 (2015) 204-214. https://doi.org/10.1016/j.memsci.2014.10.014.

[13] M.S. Suleman, K.K. Lau, Y.F. Yeong, Plasticization and swelling in polymeric membranes in CO_2 removal from natural gas, Chem. Eng. Technol., 39 (2016) 1604-1616. https://doi.org/10.1002/ceat.201500495.

[14] G.C. Kapantaidakis, G.H. Koops, M. Wessling, S.P. Kaldis, G.P. Sakellaropoulos, CO_2 Plasticization of polyethersulfone/polyimide gas-separation membranes, AIChE J., 49 (2003) 1702-1711. https://doi.org/10.1002/aic.690490710.

[15] J.K. Adewole, A.L. Ahmad, A.S. Sultan, S. Ismail, C.P. Leo, Model-based analysis of polymeric membranes performance in high pressure CO_2 removal from natural gas, J. Polym. Res., 22 (2015) 1-10. https://doi.org/10.1007/s10965-015-0658-x.

[16] A. Ebadi Amooghin, H. Sanaeepur, M. Zamani Pedram, M. Omidkhah, A. Kargari, New advances in polymeric membranes for CO_2 separation, in: A. Méndez-Vilas, A. Solano-Martín (Eds.) Polymer science: research advances, practical applications and educational aspects, Formatex Research Center, Badajoz, Spain, 2016, pp. 354-368.

[17] W.J. Koros, R.T. Chern, V. Stannett, H.B. Hopfenberg, A model for permeation of mixed gases and vapors in glassy polymers, J. Polym. Sci. B Polym. Phys., 19 (1981) 1513-1530. https://doi.org/10.1002/pol.1981.180191004.

[18] J.S. Lee, W. Madden, W.J. Koros, Antiplasticization and plasticization of Matrimid® asymmetric hollow fiber membranes. Part B. Modeling, J. Membr. Sci., 350 (2010) 242-251. https://doi.org/10.1016/j.memsci.2009.12.034.

[19] E. Sada, H. Kumazawa, J.S. Wang, Permeation of binary gas mixture through glassy polymer membranes with concentration-dependent diffusivities, J. Polym. Sci. B Polym. Phys., 30 (1992) 105-111. https://doi.org/10.1002/polb.1992.090300111.

[20] T. Visser, G.H. Koops, M. Wessling, On the subtle balance between competitive sorption and plasticization effects in asymmetric hollow fiber gas separation membranes, J. Membr. Sci., 252 (2005) 265-277. https://doi.org/10.1016/j.memsci.2004.12.015.

[21] M. Saberi, S.A. Hashemifard, A.A. Dadkhah, Modeling of CO_2/CH_4 gas mixture permeation and CO_2 induced plasticization through an asymmetric cellulose acetate membrane, RSC Adv., 6 (2016) 16561-16567. https://doi.org/10.1039/C5RA23506E.

[22] M. Rezakazemi, A. Ebadi Amooghin, M.M. Montazer-Rahmati, A.F. Ismail, T. Matsuura, State-of-the-art membrane based CO_2 separation using mixed matrix membranes (MMMs): An overview on current status and future directions, Prog. Polym. Sci., 39 (2014) 817-861. https://doi.org/10.1016/j.progpolymsci.2014.01.003.

[23] A. Ebadi Amooghin, H. Sanaeepur, M. Omidkhah, A. Kargari, "Ship-in-a-bottle", a new synthesis strategy for preparing novel hybrid host-guest nanocomposites for highly selective membrane gas separation, J. Mater. Chem. A, 6 (2018) 1751-1771. https://doi.org/10.1039/C7TA08081F.

[24] H. Sanaeepur, A. Ebadi Amooghin, E. Khademian, A. Kargari, M. Omidkhah, Gas permeation modeling of mixed matrix membranes: Adsorption isotherms and permeability models, Polym. Compos., 39 (2018) 4560-4568. https://doi.org/10.1002/pc.24564.

[25] S. Mashhadikhan, A. Moghadassi, A. Ebadi Amooghin, H. Sanaeepur, Interlocking a synthesized polymer and bifunctional filler containing the same polymer's monomer for conformable hybrid membrane systems, J. Mater. Chem. A, 8 (2020) 3942–3955. https://doi.org/10.1039/C9TA13375E.

[26] H. Sanaeepur, B. Nasernejad, A. Kargari, Cellulose acetate/nano-porous zeolite mixed matrix membrane for CO_2 separation, Greenh. Gases Sci. Technol., 5 (2015) 291-304. https://doi.org/10.1002/ghg.1478.

[27] R. Barrer, J. Barrie, J. Slater, Sorption and diffusion in ethyl cellulose. Part III. Comparison between ethyl cellulose and rubber, J. Polym. Sci., 27 (1958) 177-197. https://doi.org/10.1002/pol.1958.1202711515.

[28] W. Vieth, J. Howell, J. Hsieh, Dual sorption theory, J. Membr. Sci., 1 (1976) 177-220.

[29] X. Duthie, S. Kentish, C. Powell, K. Nagai, G. Qiao, G. Stevens, Operating temperature effects on the plasticization of polyimide gas separation membranes, J. Membr. Sci., 294 (2007) 40-49. https://doi.org/10.1016/j.memsci.2007.02.004.

[30] D. Paul, D. Kemp, The diffusion time lag in polymer membranes containing adsorptive fillers, in: Journal of Polymer Science: Polymer Symposia, Wiley Online Library, 1973, pp. 79-93. https://doi.org/10.1002/polc.5070410109.

[31] M.G. Baschetti, M. De Angelis, F. Doghieri, G. Sarti, Solubility of gases in polymeric membranes, in: M.A. Galan, E.M. del Valle (Eds.) Chemical engineering: trends and developments, Wiley, Chichester (UK), 2005, pp. 41-61. https://doi.org/10.1002/0470025018.ch2.

[32] D. Paul, W. Koros, Effect of partially immobilizing sorption on permeability and the diffusion time lag, J. Polym. Sci. B Polym. Phys., 14 (1976) 675-685. https://doi.org/10.1002/pol.1976.180140409.

[33] W. Koros, Model for sorption of mixed gases in glassy polymers, J. Polym. Sci. B Polym. Phys., 18 (1980) 981-992. https://doi.org/10.1002/pol.1980.180180506.

[34] S. Stern, V. Saxena, Concentration-dependent transport of gases and vapors in glassy polymers, J. Membr. Sci., 7 (1980) 47-59. https://doi.org/10.1016/S0376-7388(00)83184-1.

[35] C.A. Scholes, G.Q. Chen, G.W. Stevens, S.E. Kentish, Plasticization of ultra-thin polysulfone membranes by carbon dioxide, J. Membr. Sci., 346 (2010) 208-214. https://doi.org/10.1016/j.memsci.2009.09.036.

[36] H. Sanaeepur, A. Kargari, B. Nasernejad, A. Ebadi Amooghin, M.R. Omidkhah, A novel Co^{2+} exchanged zeolite Y/cellulose acetate mixed matrix membrane for CO_2/N_2 separation, J. Taiwan Inst. Chem. Eng., 60 (2016) 403–413. https://doi.org/10.1016/j.jtice.2015.10.042.

[37] K.I. Okamoto, K. Tanaka, H. Kita, A. Nakamura, Y. Kusuki, Sorption and transport of carbon dioxide in a polyimide from 3, 3′, 4, 4′-biphenyltetracarboxylic dianhydride and 4, 4′-diaminodiphenyl sulfone, J. Polym. Sci. B Polym. Phys., 27 (1989) 2621-2635. https://doi.org/10.1002/polb.1989.090271305.

[38] T.T. Moore, W.J. Koros, Gas sorption in polymers, molecular sieves, and mixed matrix membranes, J. Appl. Polym. Sci., 104 (2007) 4053-4059. https://doi.org/10.1002/app.25653.

[39] H. Sanaeepur, A. Kargari, B. Nasernejad, Aminosilane-functionalization of a nanoporous Y-type zeolite for application in a cellulose acetate based mixed matrix membrane for CO_2 separation, RSC Adv., 4 (2014) 63966-63976. https://doi.org/10.1039/C4RA08783F.

[40] A. Thran, G. Kroll, F. Faupel, Correlation between fractional free volume and diffusivity of gas molecules in glassy polymers, J. Polym. Sci. B Polym. Phys., 37 (1999) 3344-3358. https://doi.org/10.1002/(SICI)1099-0488(19991201)37:23<3344::AID-POLB10>3.0.CO;2-A.

[41] H. Sanaeepur, A. Ebadi Amooghin, S. Bandehali, Theoretical gas permeation models for mixed matrix membranes, LAP LAMBERT Academic Publishing, Beau Bassin, Mauritius, 2018.

[42] S. Kanehashi, T. Nakagawa, K. Nagai, X. Duthie, S. Kentish, G. Stevens, Effects of carbon dioxide-induced plasticization on the gas transport properties of glassy polyimide membranes, J. Membr. Sci., 298 (2007) 147-155. https://doi.org/10.1016/j.memsci.2007.04.012.

[43] T. Hirose, K. Mizoguchi, Y. Naito, Y. Kamiya, Low-pressure CO_2 sorption in poly (vinyl benzoate) conditioned to high-pressure CO_2, J. Appl. Polym. Sci., 35 (1988) 1715-1724. https://doi.org/10.1002/app.1988.070350702.

[44] H. Hachisuka, Y. Tsujita, A. Takizawa, T. Kinoshita, CO_2 sorption properties and enthalpy relaxation in alternating copoly (vinylidene cyanide-vinyl acetate)s, Polymer, 29 (1988) 2050-2055. https://doi.org/10.1016/0032-3861(88)90179-6.

[45] P. Di Lena, L. Margara, Optimal global alignment of signals by maximization of Pearson correlation, Inform. Process. Lett., 110 (2010) 679-686. https://doi.org/10.1016/j.ipl.2010.05.024.

[46] R.J. Hernandez, J.R. Giacin, E.A. Grulke, The sorption of water vapor by an amorphous polyamide, J. Membr. Sci., 65 (1992) 187-199. https://doi.org/10.1016/0376-7388(92)87064-5.

[47] J.D. Wind, C. Staudt-Bickel, D.R. Paul, W.J. Koros, Solid-state covalent cross-linking of polyimide membranes for carbon dioxide plasticization reduction, Macromolecules, 36 (2003) 1882-1888. https://doi.org/10.1021/ma025938m.

[48] R.T. Chern, W.J. Koros, E.S. Sanders, R. Yui, "Second component" effects in sorption and permeation of gases in glassy polymers, J. Membr. Sci., 15 (1983) 157-169. https://doi.org/10.1016/S0376-7388(00)80395-6.

[49] N.R. Horn, D. Paul, Carbon dioxide sorption and plasticization of thin glassy polymer films tracked by optical methods, Macromolecules, 45 (2012) 2820-2834. https://doi.org/10.1021/ma300177k.

[50] B. Videki, S. Klebert, B. Pukanszky, External and internal plasticization of cellulose acetate with caprolactone: structure and properties, J. Polym. Sci. B Polym. Phys., 45 (2007) 873-883. https://doi.org/10.1002/polb.21121.

[51] A.K. Mohanty, A. Wibowo, M. Misra, L.T. Drzal, Effect of process engineering on the performance of natural fiber reinforced cellulose acetate biocomposites, Compos. A Appl. Sci. Manuf., 35 (2004) 363-370. https://doi.org/10.1016/j.compositesa.2003.09.015.